Journal of Engineering Science and Technology
Vol. 19, No. 1 (2024) 146 - 162

THERMODYNAMIC STUDY OF SILVER-CITRATE-HYDROGEN PEROXIDE SYSTEM FOR THE EXTRACTION OF SILVER FROM ELECTRONIC WASTE

NOR NABIHA MD ZAN, WAN NUR AMIRA WAN MOHD LOTFI, YUHANEES MOHAMED YUSOF*

Chemical Engineering Section, Universiti Kuala Lumpur (UniKL) Malaysian Institute of Chemical and Biochemical Engineering (MICET), Lot 1988, Kawasan Perindustrian Bandar Vendor, Simpang Ampat, Taboh Naning, 78000 Alor Gajah, Malaysia
*Corresponding Author: yuhanees@unikl.edu.my

Abstract

The use of citric acid and hydrogen peroxide solutions for the leaching of silver from electronic waste (e-waste) has become an alternative replacing the strong and harmful acids. The thermodynamic studies of pourbaix and speciation diagrams for silver in citric acid and hydrogen peroxide solutions at various concentrations were developed using Hydra-Medusa software to demonstrate the stability zones of silver(I) ion and silver in the citric acid and hydrogen peroxide solutions. The pourbaix diagram shows that the silver(I) ion species are produced below pH of 10.5 with the potential of 0.6 V in the system containing $5e^{-5}$ M silver, 0.5 M citric acid, and 1 M hydrogen peroxide. This study also investigates the efficacy of silver leaching from the computer printed circuit board using the citric acid and hydrogen peroxide solutions and found that the highest silver concentration is 0.939 mg/L with 1.5 M of citric acid, 1.5 M of hydrogen peroxide at 40 ºC and at a static condition for 2.5 hours of leaching time. Thermodynamically, silver(I) ion is reduced to form silver at the potential below 0.501 V, where the recovery of silver by electrodeposition can be conducted. This result provides a theoretical basis for the mechanism of silver leaching and the electrodeposition of silver from the citric acid and hydrogen peroxide leachate solutions.

Keywords: Leaching, Pourbaix diagram, Printed circuit boards, Silver extraction, Thermodynamic.

1. Introduction

The rapid growth of technology for electronic devices significantly impacts human daily life. The widespread increase in electronic devices also leads to a higher generation of electronic waste (e-waste). It is estimated that 53.6 million metric tonnes of e-waste have been generated in 2019 globally and is expected to reach 74.7 million metric tonnes by 2030 [1-3]. Recycling e-waste is useful since it contains precious metals, including gold (Au), silver (Ag), and palladium (Pd) [4]. This process has made the recovery of Ag from e-waste more economical than extracting from ores, with additional environmental benefits and for the sustainability of mineral supplies [4, 5]. Table 1 shows information on the amount of Ag in the printed circuit boards (PCB) found by several researchers. A typical computer PCB contains 0.16 ppm Ag, while mobile phones contain 0.21 ppm Ag, and they are different based on the types of e-waste [6].

Previous researchers also reported that the hydrometallurgy technique provides higher metal recovery due to its simplicity in product leaching [7]. This is due to the high efficiency of strong acid that acts as a leaching agent for metals from e-waste [8-13]. Regarding its acidity level, a strong oxidant is needed to achieve an acceptable amount of metal leached from e-waste. Nevertheless, strong acids like chlorine, sulphite, and Nitrogen oxide generate waste residues during leaching, harming the environment. Alternatively, the use of citric acid ($C_6H_8O_7$) to leach metals from PCB, sewage sludge and battery waste has been studied [14-17]. $C_6H_8O_7$ is a water-soluble organic acid that degrades aerobically and anaerobically.

Besides, electrodeposition is a potential process for selective metal recovery and requires low energy consumption [18]. This method is the primary process for metal recovery and purification from an aqueous solution. It requires a low chemical reagent consumption but can produce high purity metals [19]. However, there is a limited study on the recovery of Ag from $C_6H_8O_7$ and hydrogen peroxide (H_2O_2) leachate solutions using electrodeposition. The limited knowledge of the thermodynamic of the system hindered the process from being implemented. Thus, the understanding the thermodynamic of the Ag species solubility is important.

Based on the literature, the pourbaix and species distribution diagrams have been effectively applied to evaluate the Ag leaching in the Ag-S-EDTA-H_2O system, Ag-HNO_3-H_2O system, Ag-CN-H_2O system and Ag-Cl-H_2O system [20-24]. However, the thermodynamic study for Ag leaching in the $C_6H_8O_7$ and H_2O_2 solutions is still not yet established.

In this study, to ensure that the electrodeposition technique is practical, the thermodynamic of the solution was investigated to identify the possible interference in the leaching process. This work also identified some of the main reactions based on relevant E_h -pH diagrams and the distribution of species at different concentration levels. Hence, the prevailing species in the Ag leaching system of the leaching behaviour was elucidated. The viability of the Ag recovery from $C_6H_8O_7$ and H_2O_2 leachate solutions was determined from the pourbaix diagrams, which were subsequently validated by leaching experiments. Meanwhile, the results obtained from the pourbaix and speciation diagrams will provide the theoretical basis for the mechanism of Ag leaching in the $C_6H_8O_7$ and H_2O_2 leachate solutions. Furthermore, the results will contribute to understanding the Ag dissolution and guide the thermodynamic knowledge on the recovery of Ag $C_6H_8O_7$ and H_2O_2 leachate solutions by electrodeposition.

Table 1. Metals concentration (wt%) of PCB.

Amount of Ag wt%	Types of PCB	References
0.100	PCB scrap	[11]
0.330	Waste PCB	[25]
0.210	Computer PCB	[7]
0.160	Mobile phone PCB	[7]
0.138	Mobile phone PCB	[26]
0.138	Random access Memory (RAM)	[26]
0.261	Mobile phone PCB	[27]

2. Methods

This section explains the thermodynamic analysis as well as the experimental method that were conducted in this study.

2.1. Thermodynamics of Ag-$C_6H_8O_7$-H_2O_2 system

The thermodynamic of Ag leaching was analysed according to the E_h-pH and speciation diagrams. The E_h-pH diagram is also known as the pourbaix diagram, where E_h represents the oxidation-reduction potential based on the standard hydrogen potential (SHE), while pH represents the activity of the hydrogen ion (H^+, also known as a proton) [28]. These diagrams were constructed to elucidate the predominant species in the Ag leaching system. These diagrams are beneficial in determining the oxidising ability of the Ag leaching system, as well as the possible redox reactions that may occur. For the Ag-$C_6H_8O_7$-H_2O_2 system, the E_h -pH, and speciation diagrams were developed using Hydrochemical Equilibrium- Constant Database (Hydra) - Make Equilibrium Diagrams Using Sophisticated Algorithms) (Medusa) software based on equilibrium data from the Hydra-Medusa software database [29].

The software uses the algorithm created by Eriksson [30], which reduces the Gibbs free energy of a reaction in equilibrium that can take place in the aqueous leaching media and determines the prevailing species under particular solution conditions [30, 31]. The identified components based on the Ag leaching reaction have been selected from the components listed in the Hydra. After selecting the components, the Hydra generated the appropriate complexes and solid phases of the system and the corresponding equilibrium constants. In the Medusa, the E_h-pH and speciation diagrams were generated based on the predetermined leaching conditions, such as $C_6H_8O_7$ and H_2O_2 concentrations [29].

Thermodynamically, all species in solution coexist in a condition of equilibrium. Thus, their concentrations can be predicted based on equilibrium constants (K) obtained from Gibbs free energy, assuming the system current state, such as species concentration, pH, and potential (E_h) [32]. The relevant equilibrium constants for the formation of Ag complexes obtained from the Hydra database are summarised in Table 1. Development of the pourbaix and speciation distribution diagrams assume that the temperature is 25 °C, all the stable Ag solid species have been considered, and the species with no thermodynamic information from the database have not been considered.

Table 2. Reactions and equilibrium constants for the Ag-$C_6H_8O_7$-H_2O_2 system at 25 ºC [29].

Reaction	Log K (log β)
$H^+ + cit^{3-} = H(cit)^{2-}$	6.396
$2H^+ + cit^{3-} = H_2(cit)^-$	11.157
$3H^+ + cit^{3-} = H_3(cit)^-$	14.285
$Ag^+ = H^+ + AgOH$	-12.000
$Ag^+ = 2H^+ + Ag(OH)_2^-$	-24.000
$Ag^+ = e^- + Ag^{2+}$	-33.470
$2Ag^+ = 2H^+ + Ag_2O(s)$	-12.580
$2Ag^+ = 6H^+ + 4e^- + Ag_2O_3(cr)$	-112.920
$Ag^+ = 2H^+ + e^- + AgO(s)$	-29.950
$e^- + Ag^+ = Ag(cr)$	13.510
$H_2O_2 = H^+ + HO_2^-$	-11.650

2.2. Ag leaching materials

The obsolete computer PCBs were obtained from the Universiti Kuala Lumpur (UniKL) MICET Information Technology (IT) Unit. He at al. [6] investigated the distribution of precious metals contents in the RAM of the computers and found that the RAM contains more Ag than other parts. Thus, the computer part that was used in this study is the computer's RAM (later, it is mentioned as CPCB). 99.5% of $C_6H_8O_7$ and 30 wt% of H_2O_2 were used as a leaching agent for Ag leaching. Sodium hydroxide (NaOH) was used for the chemical treatment of the CPCBs [14, 21, 33]. 69 wt% of nitric acid (HNO_3) was used for leaching to obtain the reference value for Ag in CPCB. All reagents were prepared with analytical-grade chemicals and deionised water.

2.3. Ag Leaching experiment

A 500 g of CPCB was prepared by dismantling the main electronic components from the boards and crushed into smaller pieces to obtain the desired size of about 2 cm x 2 cm per piece. 5 g of cut CPCB was then weighed on the analytical balance. Chemical pre-treatment of CPCB samples were conducted using 7.0 M of NaOH. 5 g of CPCB samples were soaked for 24 hours with 7.0 M of NaOH and then rinsed using deionised water until neutral pH was reached. The reference value for the Ag content of CPCB was determined during the leaching test with HNO_3. 100 ml of 2.5 M of HNO_3 solution was prepared by diluting with distilled water at a ratio of 1:3 (25 ml of 10 M of HNO_3 + 75 ml of H_2O) and maintained at 25 ºC. The CPCB samples were then immersed in beakers and left for 2 hours. After the concentration of Ag from HNO_3 leaching was determined, the Ag leaching tests were carried out. All leaching tests were carried out in a 200 mL beaker containing the CPCB samples and 100 mL of $C_6H_8O_7$ -H_2O_2 solutions. The CPCB pieces (2 cm x 2 cm) were immersed in the solution at 25 °C for 4 hours before proceed with leaching conditions as presented in Table 3.

During the leaching of Ag, 1 mL of leachate solution was withdrawn at 10 minutes, 80 minutes, 160 minutes and 240 minutes. Factors that have been investigated for the effect of Ag leaching are $C_6H_8O_7$ concentration, H_2O_2 concentration, temperature, and static and non-static conditions. In this study, 0 rpm and 120 rpm of stirring rate were used as the level for static and non-static leaching.

The detailed parameters associated with each experiment are shown in Table 3. All leachate samples for the Ag analysis were analysed using Atomic Absorption Spectroscopy (AAS) (AAnalyst 400 Perkin Elmer). Silver nitrate ($AgNO_3$) standard solutions were prepared at 0.5 ppm, 1.0 ppm, 1.5 ppm, 2.0 ppm, and 2.5 ppm of Ag for the standard calibration of AAS. The calibration curve was conducted with R^2 = 0.999 of linearity.

Table 3. Ag leaching parameters.

Parameters	
$C_6H_8O_7$ concentration	0.5 M, 1.0 M, 1.5 M, 2.0 M
H_2O_2 concentration	0.5 M, 1.0 M, 1.5 M, 2.0 M
Temperature	25 ^OC, 40 ^OC, 50 ^OC
Stirring rate	0 rpm, 120 rpm
Leaching time	4 hours

3. Results and Discussion

The pourbaix diagram of the Ag-$C_6H_8O_7$-H_2O_2 system at different $C_6H_8O_7$ and H_2O_2 concentrations were analysed to predict the stability of the Ag in the system. The effect of the $C_6H_8O_7$ concentration, H_2O_2 concentration, leaching temperature and stirring speed are also analysed in this paper.

3.1. E_h-pH diagrams and speciation diagrams of Ag-$C_6H_8O_7$-H_2O_2 system

The thermodynamic of Ag leaching was investigated to analyse the predominant species during the leaching process and the E_h at which the electrodeposition of Ag could occur. As shown in Fig. 1, the pourbaix diagram demonstrates that the stability zone of the Ag^+ species is produced at below pH of 10.5 with the E_h of 0.501 V in the system containing $5e^{-5}$ M Ag, 0.5 M $C_6H_8O_7$, and 0.001 M H_2O_2. At pH levels above 8, Ag precipitates such as AgO and Ag_2O are stable. Meanwhile the Ag_2O_3 forms at higher E_h which is in the E_h range of 0.75 V- 1.8 V and the stability region becomes wider with an increasing of pH. Figure 2 depicts similar trends for the higher $C_6H_8O_7$ concentration. As a result, an appropriate pH range is required to avoid Ag precipitation from the solution during the leaching of Ag. The precipitation of Ag_2O and Ag_2O_3 form at higher pH and E_h [34, 35]. Besides, the equilibrium between Ag/Ag^+ is influenced by E_h. It can be observed that the oxidising of Ag^+ occurs at the E_h greater than 0.501 V. The stability of Ag^+ also declines at higher E_h and pH [33]. The figure also shows that Ag is formed when the E_h falls below 0.501 V. This result also suggests that Ag recovery by electrodeposition is possible at the applied E_h below 0.501 V, where the Ag^+ is reduced to Ag [36].

Figure 3(a) depicts the influence of pH on the speciation of Ag complex species at the E_h of 0.6 V. It demonstrates that by keeping the E_h at 0.6 V, the generation of Ag_2O precipitate in the pH range of 10.8 - 12 can be prevented [37]. As shown in Fig. 3(b), at the pH range of 10.8 - 12, the predominant species is Au^+ even though the fraction is declining above pH of 10 and approximately, 0.88 fraction of Ag_2O presents at pH of 12. This figure supports the view that Ag^+ is the dominant species at pH of 5 and is consistent with the pourbaix diagrams shown in Figs. 1 and 2. Thus, the recovery of Ag from the leachate solution by electrodeposition is feasible when there is no precipitation of Ag forms in the leachate solution. The influence of the E_h on the speciation of Ag complex species at a pH of 5.0 is demonstrated in Fig. 4. In this figure, Ag^+ can be formed between 0.6 V and 1.3 V without precipitation. Thus, to avoid the precipitation of Ag_2O, pH of 5 was selected to leach Ag from $C_6H_8O_7$ and H_2O_2 solutions. At this region, the leaching of Ag from CPCB is feasible, and the Ag is fully oxidised to Ag^+ during the leaching process [21].

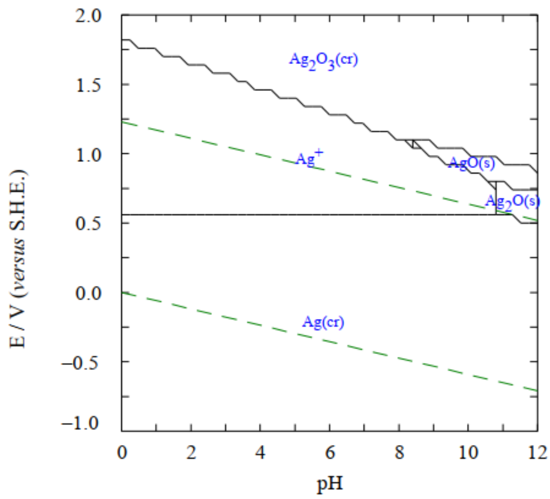

Fig. 1. E_h-pH diagram of Ag-$C_6H_8O_7$-H_2O_2 system.
Conditions: Ag $5x10^{-5}$ M, $C_6H_8O_7$ 0.5 M, H_2O_2 0.001 M.

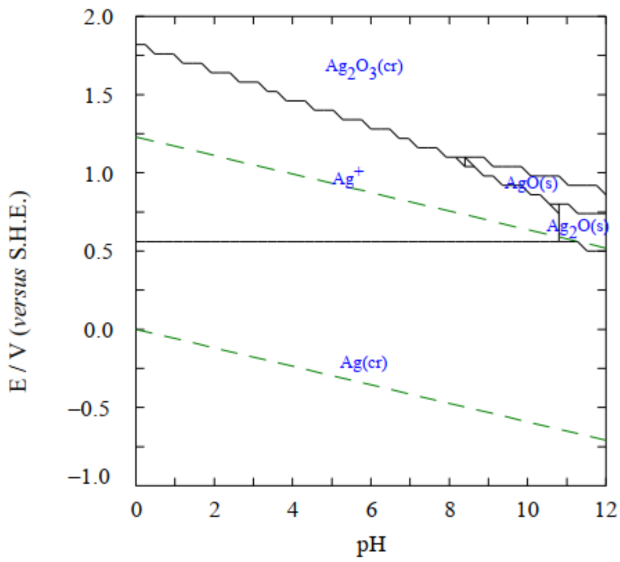

Fig. 2. E_h-pH diagram of Ag-$C_6H_8O_7$-H_2O_2 system.
Conditions: Ag $5x10^{-5}$ M, $C_6H_8O_7$ 1.5 M, H_2O_2 0.075 M.

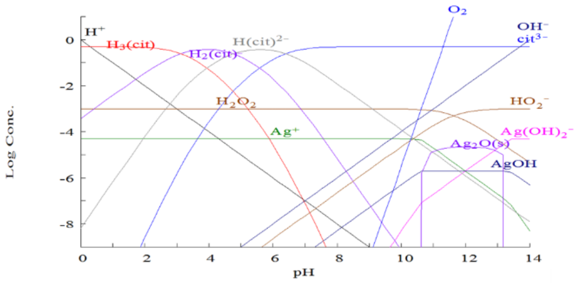

(a)

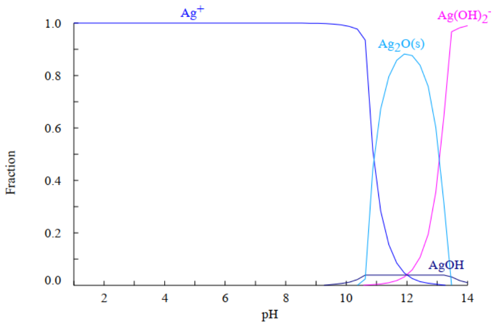

(b)

Fig.3. (a). Log concentration of Ag species in the Ag-$C_6H_8O_7$-H_2O_2 system. Condition: E_h = 0.6 V, (b)Fraction of Ag species in the Ag-$C_6H_8O_7$-H_2O_2 system. Condition: E_h = 0.6 V.

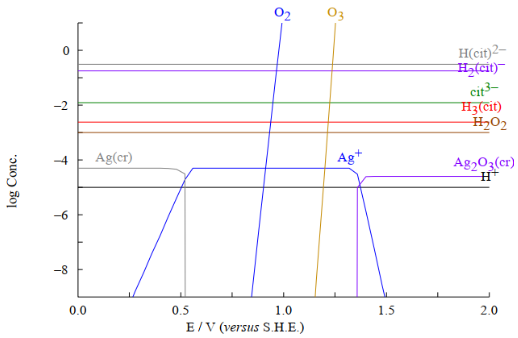

Fig. 4. Distribution of Ag species in Ag-$C_6H_8O_7$-H_2O_2 system. Condition: pH = 5.

Figures 5 and 6 depict the Ag speciation diagrams of Ag-$C_6H_8O_7$ - H_2O_2 at 0.5 M and 2.0 M $C_6H_8O_7$, respectively. It can be seen that the compound generated when Ag is leached at pH of 5 was comparable. At this pH, the distribution of Ag^+ for both $C_6H_8O_7$ concentrations show a similar trend. The result shows that increasing the reagent concentration did not increase the Ag leaching [22]. Increasing the $C_6H_8O_7$ concentration causes simultaneous reaction, such as precipitation of copper (Cu) oxides forming on the Ag surface [22]. Another reason for this is due to the dissolution of other metals, such as lead (Pb) and zinc (Zn), that oxidised during the leaching of CPCB using $C_6H_8O_7$ and H_2O_2 solutions as these metals have wider and lower oxidising E_h than Ag [38]. Figure 7 depicts the behaviour of the Ag-$C_6H_8O_7$ - H_2O_2 system when the concentration of H_2O_2 is raised to 1 M. It can be seen in the figure that the increase of H_2O_2 has no effect on the distribution of the Ag^+. This thermodynamic prediction is supported by result from a previous study where the increase of H_2O_2 concentration has no significant effect on Ag leaching [14]. Besides, the dissolution of Cu may also occur, and $Cu(H_2Cit)^+$ becomes the predominant species at pH of 5 [39]. The dissolution of Ag in the H_2O_2 is shown in the following reactions [14].

$$\mathrm{Ag(s) + H_2O_2(aq) \rightarrow Ag^+(aq) + OH + OH^-} \tag{1}$$

$$\mathrm{Ag(s) + OH \rightarrow Ag^+(aq) + OH^-} \tag{2}$$

According to Jadhav et al. [14], the concentration of $C_6H_8O_7$ has no impact on the leaching of Ag. The dissolution of Ag with organic acid was due to the dissolution of organic acid that produce protons and ligands, as shown in Equation 3. The reduction of protons generates hydrogen and oxidise the metal, as shown in Eqs. 4 and 5 [14].

$$\mathrm{RCOOH\ +\ H_2O\ \leftrightarrow RCOO^-\ +\ H_3O^+} \tag{3}$$

$$\mathrm{2H_3O^+ + 2e^- \rightarrow H_2 + H_2O} \tag{4}$$

$$\mathrm{M \rightarrow + M^{2+} + 2e^-} \tag{5}$$

where M is the metal.

Organic acid complexing mechanisms create stable metal complexes, and the resulting reaction makes the metals in the solution more stable [40]. The mixture of $C_6H_8O_7$ and H_2O_2 solutions enhanced the leaching of Ag due to the presence of peroxy carboxylic and H_2O_2. The reaction of $C_6H_8O_7$ and H_2O_2 during the dissolution of Ag produced $Ag(C_6H_6O_7)$ is proposed based on the mechanism suggested by Jadhav et al [14], as shown in Equation 6. This reaction shows that the precipitation of $Ag(C_6H_6O_7)$ also may form during the leaching of Ag in the $C_6H_8O_7$ and H_2O_2 solutions [41]. The formation of $Ag(C_6H_6O_7)$ in the solution limits the dissolution of Ag to further form during the leaching process [41].

$$\mathrm{C_6H_8O_7 + Ag + H_2O_2 \rightarrow Ag(C_6H_6O_7) +\ H_2O + Ag^+} \tag{6}$$

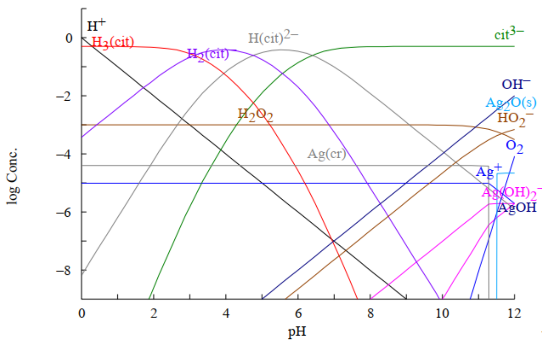

Fig. 5. Speciation diagram of Ag leaching for Ag 5x10^{-5}M- $C_8H_7O_7$ 0.5M- H_2O_2 0.001M.

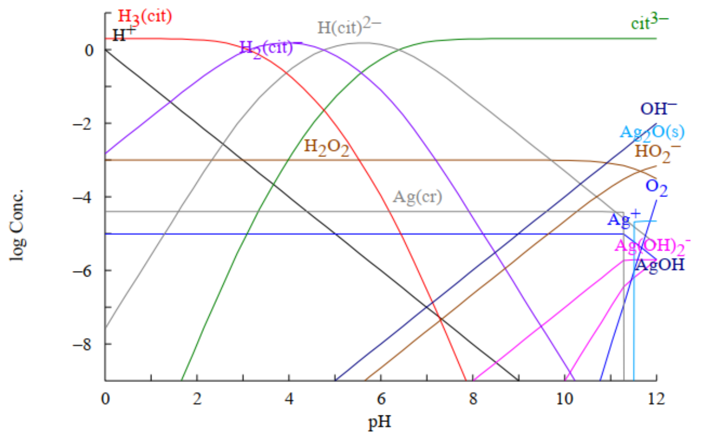

Fig. 6. Speciation diagram of Ag leaching for Ag 5x10^{-5}M- $C_8H_7O_7$ 2.0 M- H_2O_2 0.001M.

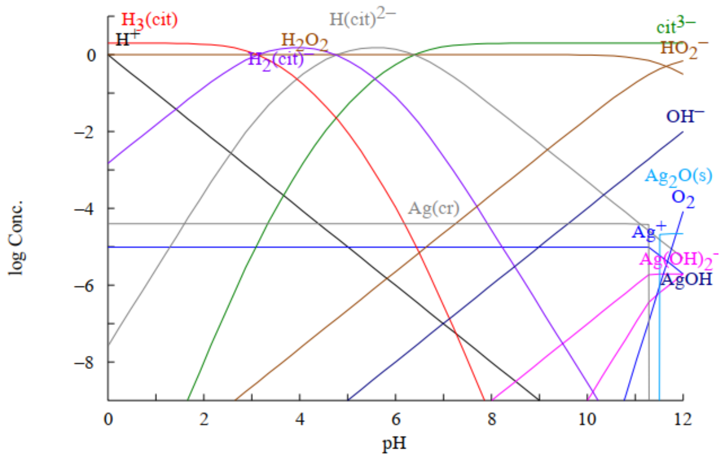

Fig.7. Speciation diagram of Ag leaching for Ag 5x10^{-5}M- $C_8H_7O_7$ 2.0 M- H_2O_2 1.0 M.

3.2. Leaching of Ag from CPCB using $C_8H_7O_7$- H_2O_2 solutions.

The effect of CPCB pre-treatment with NaOH was examined. Figure 8 illustrates the difference of Ag concentration with and without a 7.0 M NaOH pre-treatment. After the CPCB was pre-treated using NaOH, the CPCB was leached using HNO_3 to determine the reference concentration of Ag in the CPCB. The highest concentration of Ag achieved in this study was compared to the reference value, the percentage of Ag was calculated based on the equation below:

$$\frac{silver\ concentration}{silver\ reference\ concentration}\ x\ 100\% \tag{7}$$

In this study, the concentration of Ag was measured every 1 hour to examine the Ag leaching trend during the pre-treatment of CPCB. The result also shows that, 1 hour interval is sufficient as a significant trend was obtained for Ag leaching. It can be seen that both conditions show the increasing of Ag concentration in the first hour of leaching, with 3.625 mg/L and 3.15 mg/L of Ag leached with and without pre-treatment, respectively. However, as the time increased, only the pre-treated sample shows a gradual increase of the Ag concentration, and after 3 hours, 5.945 mg/L of Ag is successfully leached. Thus, 5.945 mg/L was selected as the reference value for Ag in the CPCB sample. According to Adhapure et al. [33], the presence of solder coating on the CPCB limited the leaching of metals and can be removed by using NaOH. Similarly, Jadhav et al. [14] used NaOH to pretreat the CPCB and found that the chemical coating was fully removed. In this study, a similar method was employed, resulting in the chemical coating on the CPCB sample being fully removed after the pre-treatment. The quantity of Ag lost during the pre-treatment process was less than 1mg/L based on the AAS analysis. The result indicates that pre-treatment is required for the Ag leaching from CPCB as the chemical coating that covered the metals hindered the leaching of metals on the PCB [14, 33].

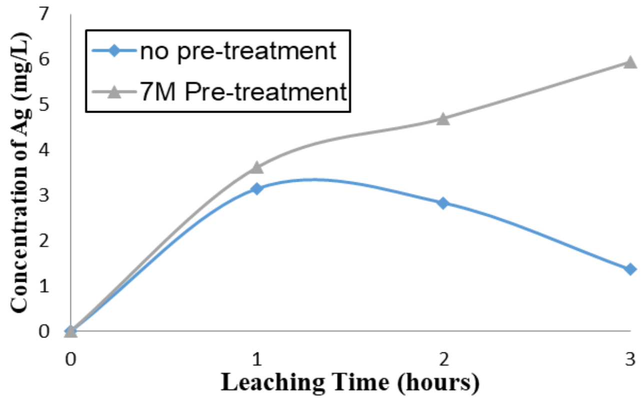

Fig. 8. Chemical pre-treatment of CPCB.

The concentrations of $C_6H_8O_7$ were varied at 0.5 M, 1.0 M, 1.5 M, and 2.0 M with a constant H_2O_2 concentration of 1.5 M. The pH was kept acidic, and the leaching duration was 4 hours. The effect of $C_6H_8O_7$ concentrations on Ag leaching was studied. As shown in Fig. 9, the concentration of Ag increased steeply for the first 10 minutes and then decreased gradually until 80 minutes for all $C_6H_8O_7$ concentrations. The Ag concentration was constant for 0.5 M and 1.0 M $C_6H_8O_7$ concentrations until 240 minutes. However, the concentration of Ag continued to increase for 1.5 M and 2.0 M $C_6H_8O_7$ concentration as the leaching time increased from 80 minutes until 160 minutes. At 160 minutes, the highest Ag concentration was obtained for 1.5 M $C_6H_8O_7$ concentration (0.822 mg/L), but the concentration of Ag leaching reduced until 240 minutes.

The decrease of Ag concentration during the leaching test was due to the formation of hydroxide precipitate on the surface of Ag. However, a complete Ag leaching was achieved in 240 minutes for all $C_6H_8O_7$ concentrations used. This is because the concentration of H_2O_2 used has been maintained. Thus, the amount of peroxy carboxylic acid formed remain constant regardless of $C_6H_8O_7$ concentration. Nevertheless, excessive $C_6H_8O_7$ concentration may result in a rise in byproduct that promotes the synthesis of the metal hydrogen citrate [14]. Given this result, 1.5 M of $C_6H_8O_7$ was used in further leaching experiments.

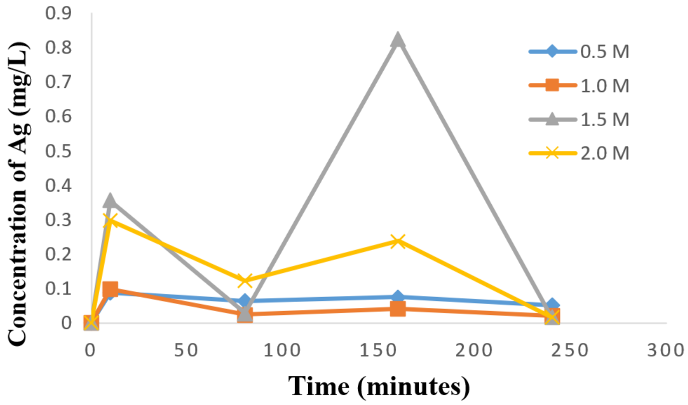

Fig. 9. Ag leaching at various $C_6H_8O_7$ concentrations with constant H_2O_2 concentration of 1.5 M.

The influence of H_2O_2 concentrations was studied during the Ag leaching experiment with $C_6H_8O_7$ as the leaching agent. The initial concentration of H_2O_2 were controlled at 0.5 M, 1.0 M, 1.5 M, and 2.0 M. As shown in Fig. 10, as the time increased, it can be observed that the concentration of Ag leaching is increased until 80 minutes for H_2O_2 concentrations of 0.5 M, 1.5 M, and 2.0 M. However, the Ag concentration of 1.0 M H_2O_2 continued to drop after 80 minutes until 240 minutes. The highest Ag concentration was obtained at 1.5 M H_2O_2 (0.146 mg/L). The result found that 1.5 M of H_2O_2 was sufficient to enhance the dissolution of Ag. However, previous study suggested that the leaching of Ag was effective with the addition of H_2O_2 that can help to improve the efficiency of Ag leaching [15, 17].

According to Jadhav et al., [14], the concentration of Ag was maintained as the H_2O_2 concentration increased to 7%. Nevertheless, in this study, a lower Ag concentration was obtained as the $C_6H_8O_7$ concentration increased to 2.0 M. This result was also shown in previous study that a decrease of Ag leaching is due to the precipitation of other dissolved metals, such as copper oxides, which reduce the ability of Ag dissolution [22].

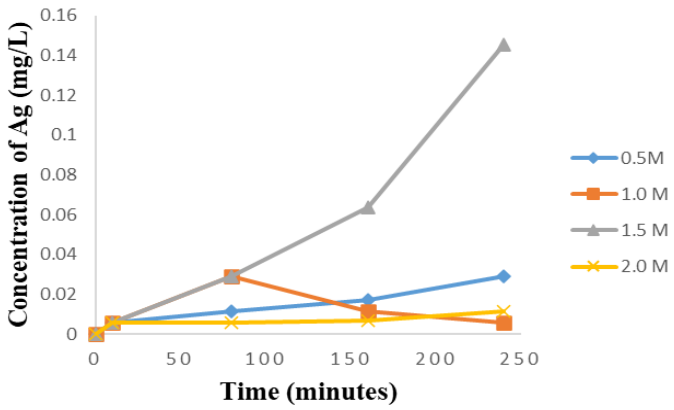

Fig. 10. Ag leaching at various H_2O_2 concentrations with constant $C_6H_8O_7$ at 1.5 M.

Figure 11 shows the effect of reaction temperatures on the leaching of Ag at 1.5 M $C_6H_8O_7$ and 1.5 M H_2O_2. The trend in Fig. 11 demonstrates an increasing trend at all temperatures peaked at 80 minutes with the highest at 40 °C (0.700 mg/L). With further leaching, it appears that the concentration of Ag at 25 ˚C and 40 °C temperatures are decreased. Comparing the concentration of Ag obtained, increasing the temperature to 50 ˚C reduced the Ag leaching. This is because further leaching of Ag leads to the formation of competing reactions, such as the as silver oxide (Ag_2O) and silver hydroxide (AgOH) precipitates, resulting in the decrease of Ag^+ concentration in the solution [42]. This is in line with the result obtained from Meshram et. al [43], where the leaching of metals decreases at higher temperatures. A similar trend was observed in a study from Gargul et al. [44], where they found a decrease in the leaching of lead (Pb) and Cu with $C_6H_8O_7$ at higher temperatures.

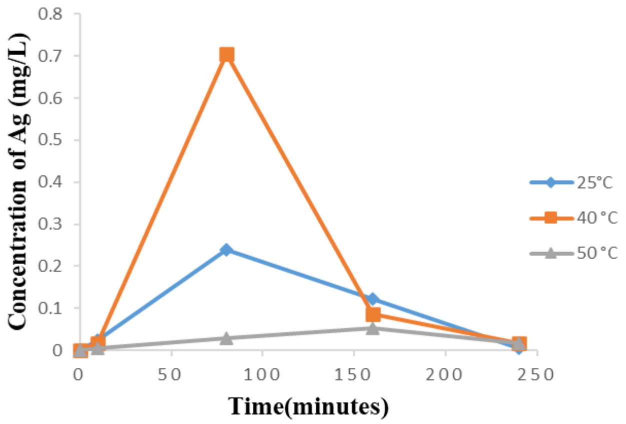

Fig. 11. Ag leaching at various temperatures at1.5 M $C_6H_8O_7$ and 1.5 M H_2O_2.

Figure 12 shows the effect of the stirring rates on the leaching of Ag at 1.5 M $C_6H_8O_7$ and 1.5 M of H_2O_2. Leaching experiments compared the Ag leaching with stirring conditions at 120 rpm and without stirring. Initially, both experiments demonstrated that the Ag leaching was low for 80 minutes. At 160 minutes, 0.939 mg/L Ag was successfully obtained at the static condition and lower Ag concentration was obtained at 120 rpm. However, the leaching of Ag at both conditions were declined after 160 minutes. In contrast to these findings, Jadhav et al. [14] demonstrated that stirring speed had no influence on metal leaching, with results demonstrating that 100% of metal leaching was achieved at a static condition and 150 rpm. The decrease of Ag leaching suggested that the stirring speed has negatively impacted the metal leaching process. This is because the degradation of H_2O_2 at high stirring speed causes excessive oxygen on the particle surface, inhibiting the reaction between metal and peroxide [45, 46]. In addition, the excessive amount of oxygen promotes the formation of Ag_2O precipitate during the leaching process decreasing the Ag^+ in the solution [47]. The highest concentration of Ag achieved in this study was 0.939 mg/L and this concentration was compared to the Ag leaching with HNO_3. It shows that approximately 15.8% of Ag was successfully obtained from CPCB samples. However, the feasibility of leaching of Ag using $C_6H_8O_7$ and H_2O_2 solutions cannot be neglected. Thus, the optimisation study of the Ag leaching parameters using Design of Experiments (DOE) technique is recommended for future study.

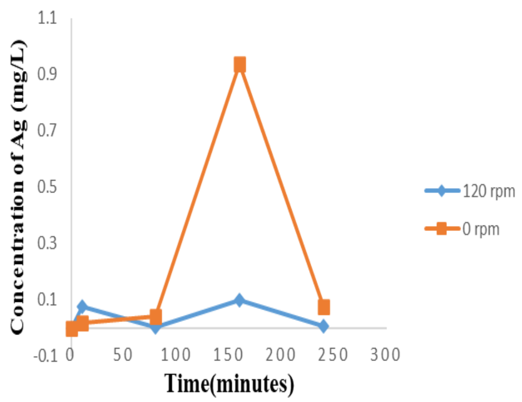

Fig. 12. Ag leaching with string and without stirring.

4. Conclusions

In this study, E_h-pH and species distribution diagrams under various conditions of pH, E_h and concentrations of $C_6H_8O_7$ and H_2O_2 were developed to evaluate the thermodynamic of Ag leaching and recovery in $C_6H_8O_7$ and H_2O_2 solutions.

From the pourbaix diagram developed by the Hydra-Medusa software, the variations in concentrations of $C_6H_8O_7$ and H_2O_2 have no discernible effect on the Ag^+ species formed. The speciation diagram shows that the predominance species during the Ag leaching is Ag^+ at 0.6 V and pH of 5, and this finding was validated during the leaching experiments.

The results obtained from the leaching of Ag using $C_6H_8O_7$ and H_2O_2 solutions show that the leaching condition with 1.5 M of $C_6H_8O_7$, 1.5 M of H_2O_2 at 40°C and at a static condition for 160 minutes of leaching time produce the highest Ag concentration which is 0.939 mg/L. Even though, the concentration of Ag leaching is far from the concentration of Ag leaching using HNO_3, the feasibility of $C_6H_8O_7$ and H_2O_2 solutions to leach Ag is undenied. Future investigation can be undertaken to explore the optimum parameters using DOE technique for Ag leaching from e-waste using $C_6H_8O_7$ and H_2O_2 solutions.

Thermodynamically, the result suggested that the recovery of Ag from $C_6H_8O_7$ and H_2O_2 leachate solution is possible at the E_h below 0.501 V and at pH < 10.5, where at this condition, the Ag^+ is reduced to form Ag. Thus, the recovery of Ag from $C_6H_8O_7$ and H_2O_2 leachate solutions using electrodeposition is feasible. This finding provides a theoretical basis for the electrodeposition of Ag from the $C_6H_8O_7$ and H_2O_2 leachate solutions, especially for the recovery of Ag from e-waste. As a future recommendation, the study of electrodeposition of Ag from $C_6H_8O_7$ and H_2O_2 leaching solution should be conducted.

Acknowledgements

The authors would like to thank to the UniKL MICET for financially support this research from the Short-Term Research Grant (STRG) (str19037). The authors also gratefully acknowledge use of services and facilities of UniKL MICET. The technical assistance received from the staffs of the laboratories are greatly appreciated.

Nomenclatures

E_h	Potential
K	Equilibrium constant
M	Metal

Greek Symbols

β	Overall equilibrium constant

Abbreviations

AAS	Atomic Absorption Spectroscopy
Ag	Silver
$Ag(C_6H_6O_7)$	Silver hydrogen citrate
$AgNO_3$	Silver nitrate
AgO	Silver(I) oxide
Ag_2O	Silver(II) oxide
Ag_2O_3	Silver(III) oxide
AgOH	Silver hydroxide
Au	Gold
$C_6H_8O_7$	Citric acid
Cl	Chloride
CN	Cyanide
CPCB	Computer Printed Circuit Boards
Cu	Copper
DOE	Design of Experiments
EDTA	Ethylenediaminetetraacetic acid
H	Hydrogen
HNO_3	Nitric acid
H_2O_2	Hydrogen peroxide
H_2O	Water
IT	Information Technology
MICET	Malaysian Institute of Chemical and Bioengineering Technology
NaOH	Sodium Hydroxide
Pb	Lead
Pd	Palladium
PCB	Printed circuit boards
RAM	Random access Memory
S	Sulphur
SHE	Standard hydrogen electrode
Zn	Zinc

References

1. Rene, E.R.; Sethurajan, M.; Kumar Ponnusamy, V.; Kumar, G.; Bao Dung, T.N.; Brindhadevi, K.; and Pugazhendhi, A. (2021). Electronic waste generation, recycling, and resource recovery: Technological perspectives and trends. *Journal of Hazardous Materials*, 416, 125664.
2. Forti, V.; Balde, C.P.; Kuehr, R.; and Bel, G. (2020). The global E-waste monitor 2020: Quantities, flows and the circular economy potential. United

Nations University (UNU) / United Nations Institute for Training and Research (UNITAR) - co-hosted SCYCLE Programme, International Telecommunication Union (ITU) & International Solid Waste Association (ISWA), Bonn/Geneva/Rotterdam.

3. Huisman, J.; Stevels, A.; Baldé, K.; Magalini, F.; and Kuehr, R. (2019). The e-waste development cycle - part i, introduction and country status. *Waste Electrical and Electronic Equipment (WEEE) Handbook (Second Edition)*. Woodhead Publishing Series in Electronic and Optical Materials, 17-55.
4. Balde, C.P.; Forti, V.; Gray, V.; Kuehr, R.; and Stegmann, P. (2017). The global e-waste monitor 2017. United Nations University (UNU), International Telecommunication Union (ITU) & International Solid Waste Association (ISWA), Bonn/Geneva/Vienna.
5. Zeng, X.; Mathews, J.A.; and Li, J. (2018). Urban mining of E-waste is becoming more cost-effective than virgin mining. *Environmental Science and Technology*, 52(8), 4835-4841.
6. He, J.; Yang, J.; Tariq, S.M.; Duan, C.; and Zhao, Y. (2020). Comparative investigation on copper leaching efficiency from waste mobile phones using various types of ionic liquids. *Journal of Cleaner Production*, 256, 120368.
7. Yamane, L.H.; de Moraes, V.T.; Espinosa, D.C.R.; and Tenório, J.A.S. (2011). Recycling of WEEE: Characterization of spent printed circuit boards from mobile phones and computers. *Waste Management*, 31(12), 2553-2558.
8. Elshehy, E.A.; Shenashen, M.A.; Abd El-Magied, M.O.; Tolan, D.A.; El-Nahas, A.M.; Halada, K.; Atia, A.A.; and El-Safty, S.A. (2017). Selective recovery of silver(i) ions from e-waste using cubically multithiolated cage mesoporous monoliths. *European Journal of Inorganic Chemistry*, 2017(41), 4823-4833.
9. Li, H.; Eksteen, J.; and Oraby, E. (2018). Hydrometallurgical recovery of metals from waste printed circuit boards (WPCBs): Current status and perspectives - A review. *Resources, Conservation and Recycling*, 139, 122-139.
10. Akcil, A.; Erust, C.; Gahan, C.S.E.; Ozgun, M.; Sahin, M.; Tuncuk, A. (2015). Precious metal recovery from waste printed circuit boards using cyanide and non-cyanide lixiviants-A review. *Waste Management*, 45, 258-271.
11. Park, Y.J.; and Fray, D.J. (2009). Recovery of high purity precious metals from printed circuit boards. *Journal of Hazardous Materials*, 164(2-3), 1152-1158.
12. Tuncuk, A.; Stazi, V.; Akcil, A.; Yazici, E.Y.; and Deveci, H. (2012). Aqueous metal recovery techniques from e-scrap: Hydrometallurgy in recycling. *Minerals Engineering*, 25(1), 28-37.
13. Yang, H.; Liu, J.; and Yang, J. (2011). Leaching copper from shredded particles of waste printed circuit boards. *Journal of Hazardous Materials*, 187(1-3), 393-400.
14. Jadhav, U.; Su, C.; and Hocheng, H. (2016). Leaching of metals from large pieces of printed circuit boards using citric acid and hydrogen peroxide. *Environmental Science and Pollution Research*, 23, 24384-24392.
15. Li, L.; Ge, J.; Wu, F.; Chen, R.; Chen, S.; and Wu, B. (2010). Recovery of cobalt and lithium from spent lithium ion batteries using organic citric acid as leachant. *Journal of Hazardous Materials*, 176(1-3), 288-293.
16. Sonmez, M.S.; and Kumar, R.V. (2009). Leaching of waste battery paste components. Part 1: Lead citrate synthesis from PbO and PbO_2. *Hydrometallurgy*, 95(1-2), 53-60.

17. Li, L.; Ge, J.; Chen, R.; Wu, F.; Chen, S.; and Zhang, X. (2010). Environmental friendly leaching reagent for cobalt and lithium recovery from spent lithium-ion batteries. *Waste Management*, 30(12), 2615-2621.
18. Tanong, K.; Tran, L. H.; Mercier, G.; and Blais, J. F. (2017). Recovery of Zn (II), Mn (II), Cd (II) and Ni (II) from the unsorted spent batteries using solvent extraction, electrodeposition and precipitation methods. *Journal of Cleaner Production*, 148, 233-244.
19. Jin, W.; Hu, M.; and Hu, J. (2018). Selective and efficient electrochemical recovery of dilute copper and tellurium from acidic chloride solutions. *ACS Sustainanble Chemistry Engineering*, 6(10), 13378-13384.
20. Puente-Siller, D. M.; Fuentes-Aceituno, J. C.; and Nava-Alonso, F. (2013). A kinetic-thermodynamic study of silver leaching in thiosulfate-copper-ammonia-EDTA solutions. *Hydrometallurgy*, 134-135, 124-131.
21. Martinez-Ballesteros, G.; Valenzua-Garcia, J.L.; Gomez-Alvarez, A.; Encinas-Romero, M.A.; Mejia-Zamudio, F. A.; Rosas-Durazo, A.D.; Valenzuele-Frisby, R. (2021). Recovery of ag, au, and pt from printed circuit boards by pressure leaching. *Recycling*, 6(4), 67, 1-13.
22. Barragan, J. A.; Ponce De León, C.; Alemán Castro, J. R.; Peregrina-Lucano, A.; Gómez-Zamudio, F.; and Larios-Durán, E. R. (2020). Copper and antimony recovery from electronic waste by hydrometallurgical and electrochemical techniques. *ACS Omega*, 5(21), 12355-12363.
23. Oudbashi, O.; and Wanhill, R. (2021). Long-term embrittlement of ancient copper and silver alloys. *Heritage*, 4(3), 2287-2319.
24. Reyes-Cruz, V.; Ponce-de-León, C.; González, I.; and Oropeza, M. T. (2002). Electrochemical deposition of silver and gold from cyanide leaching solutions. *Hydrometallurgy*, 65(2-3), 187-203.
25. Huang, K.; Guo, J.; and Xu, Z. (2009). Recycling of waste printed circuit boards: A review of current technologies and treatment status in China. *Journal of Hazardous Materials*, 164(2-3), 399-408.
26. Sahin, M.; Akcil, A.; Erust, C.; Altynbek, S.; Gahan, C.S.; and Tuncuk, A. (2015). A potential alternative for precious metal recovery from E-waste: iodine leaching. *Separation Science and Technology*, 50(16), 2587-2595.
27. Ding, Y.; Zhang, S.; Liu, B.; Zheng, H.; Chang, C.C.; and Ekberg, C. (2019). Recovery of precious metals from electronic waste and spent catalysts: A review. *Conservation and Recycling*, 141, 284-298.
28. Huang, H.-H. (2016). The Eh-pH diagram and its advances. *Metals*, 6(1), 23.
29. Puigdomenech, I. (2020). HYDRA (Hydrochemical equilibrium- constant database) and MEDUSA (Make equilibrium diagrams using sophisticated algorithms) programs. *Royal Institute of Technology, Sweden*, Retrived January 31, 2020, from http://www.kemi.kth.se/medusa/.
30. Eriksson, G. (1979). An algorithm for the computation of aqueous multi-component, multiphase equilibria. *Analytica Chimica Acta*, 112(4), 375-383.
31. Petter, P.M.H.; Veit, H.M.; and Bernardes, A.M. (2014). Evaluation of gold and silver leaching from printed circuit board of cellphones. *Waste Management*, 34(2), 475-482.
32. Liu, X.; Xu, B.; Yang, Y.; Li, Q.; Jiang, T.; and He, Y. (2018). Thermodynamic analysis of ammoniacal thiosulphate leaching of gold catalysed by Co(III)/Co(II) using Eh-pH and speciation diagrams. *Hydrometallurgy*, 178, 240-249.

33. Adhapure, N.N.; Dhakephalkar, P.K.; Dhakephalkar, A.P.; Tembhurkar, V.R.; Rajgure, A.V.; and Deshmukh, A.M. (2014). Use of large pieces of printed circuit boards for bioleaching to avoid 'precipitate contamination problem' and to simplify overall metal recovery. *MethodsX*, 1, 181-186.
34. Hans, M.; Mathews, S.; Mücklich, F.; and Solioz, M. (2016). Physicochemical properties of copper important for its antibacterial activity and development of a unified model, *Biointerphases*, 11(1): 018902.
35. Manzano, C.V.; Llorente del Olmo, C.; Caballero-Calero, O.; and Martín-González, M. (2021). High thermoelectric efficiency in electrodeposited silver selenide films: From Pourbaix diagram to a flexible thermoelectric module. *Sustainable Energy & Fuels*, 5(18), 4597-4605.
36. Fukui, R.; Katayama, Y.; and Miura, T. (2010). The influence of potential under diffusion-controlled region on electrodeposition of silver in an amide-type ionic liquid. *ECS Transactions*, 33(7), 555-561.
37. Lyon, S.B.(2010). Corrosion of noble metals. *Shreir's Corrosion*,1, 2205-2223.
38. Borda, J.; González, C.; and Torres, R.(2023). Aqueous recovery of zinc and lead from coal fly ashes of a colombian thermoelectric plant. *Ingenieria e Investigacion*, 43(1), e95364, 1-8.
39. Cadien, K. C.; Nolan, L. (2012). *7-CMP method and practice*. (3rd ed.). Handbook of Thin Film Deposition,, 179-219.
40. Segura-Bailón, B.; and Lapidus, G.T. (2021). Selective recovery of copper contained in waste PCBs from cellphones with impurity inhibition in the citrate-phosphate system. *Hydrometallurgy*, 203, 105699.
41. Djokić, S. (2008). Synthesis and antimicrobial activity of silver citrate complexes. *Biorganic Chemistry and Appliations*, Volume 2008, Article ID 436458.
42. Starovoytov, O.N.; Kim, N.S.; Han, K.N. (2007). Dissolution behavior of silver in ammoniacal solutions using bromine, iodine and hydrogen-peroxide as oxidants. *Hydrometallurgy,* 86(1-2), 114-119.
43. Meshram, P.; Bhagat, L.; Prakash, U.; Pandey, B. D.; and Abhilash (2017). Organic acid leaching of base metals from copper granulated slag and evaluation of mechanism. *Canadian Metallurgy Quarterly*, 56(2), 168-178.
44. Gargul, K.; Boryczko, B.; Bukowska, A.; Jarosz, P.; and Małecki, S.(2019). Leaching of lead and copper from flash smelting slag by citric acid. *Archives of Civil and Mechanical Engineering*, 19(3), 648-656.
45. Birloaga, I.; De Michelis, I.; Ferella, F.; Buzatu, M.; Vegliò, F. (2013). Study on the influence of various factors in the hydrometallurgical processing of waste printed circuit boards for copper and gold recovery. *Waste Management*, 33(4), 935-941.
46. Ajiboye, E.A.; Panda, P.K.; Adebayo, A.O.; Ajayi, O.O.; Tripathy, B.C.; Ghosh, M.K.; Basu, S. (2019). Leaching kinetics of Cu, Ni and Zn from waste silica rich integrated circuits using mild nitric acid. *Hydrometallurgy*, 188, 161-168
47. Pourbaix, M. (1958). Atlas of electrochemical equilibria in aqueous solutions. Pergamon.